Doctoral School on Engineering Sciences
Università Politecnica delle Marche

Extended summary

# Studio di una frana in terreni strutturalmente complessi: interazione con le opere di imbocco di una galleria stradale

*Curriculum: Ingegneria dei materiali, delle acque e dei terreni*

Author

Alessandro Vita

Tutor

Giuseppe Scarpelli

Date: 30 January 2012

---

**Abstract**. During the construction of the south portal of the tunnel Baldaia I along the SS106 motorway in Calabria, unexpectedly large and continuous displacements of the earth retaining structures occurred leading to a precautionary suspension of the excavation works. To study the kinematics of the observed instability phenomenon, inclinometer probes were used together with the topographic monitoring of the portal structures; it was found that the unstable mechanism was deep-seated, block-type and extending over the entire slope. In this paper the site investigation activities carried out to understand the origin of the instability process are presented. The interpretation of the observed behaviour is then given together with the description of the remedial measures suggested to safely complete the construction of the tunnel. The link between the time evolution of the instability and the sequence of the excavation works, which turned out to be an important issue in the process, is also discussed in some detail.

**Keywords.** Slope instability, stiff clays, earth retaining structures, tunnelling.

# 1 Introduction

The DG21/04 maxi-section constitutes part of the SS106 Jonica national road construction plan which covers a road segment about 17 km long, from the town of Squillace to the Simeri Crichi junction. The works will lead to the development of a new dual carriage highway system, connecting Taranto to Reggio Calabria along the Ionian coastline. Due to the morphology of the selected layout, the general plans included many tunnels in order to reduce the average slope of the road. Typically, short length low-cover dual tunnels, one for each carriageway, are employed; their horizontal span is of 14.0 m and the vertical span of 12.0 m, with a gross excavation area of 130 m2. Due to the high number of tunnel portals to be excavated, the construction of the road entails important modifications of the local slope morphology. The geological area involved is the so called “Catanzaro Basin” which is apparently constituted by the uniform marine formations belonging to the pliocenic cycle (mainly silty clays interlayered by conglomeratic sandstone); however, these formations are characterized by the marked presence of tectonic structures. Such highly tectonized areas are landslide-prone and often give rise to extended failures even for excavations of small extent.

In April 2008, during the construction of the south portal of the Baldaia I tunnel, an unexpectedly large and continuous displacement of the earth retaining structures caused a long suspension of the works that was resolved only after a new design and a change in the construction strategy of the tunnel were introduced.

# 2 Case description

## 2.1 The site

The Baldaia I south portal is located halfway up a concave slope dipping about 20° ESE, on the left side of the Fiasco torrent (Fig. 1).

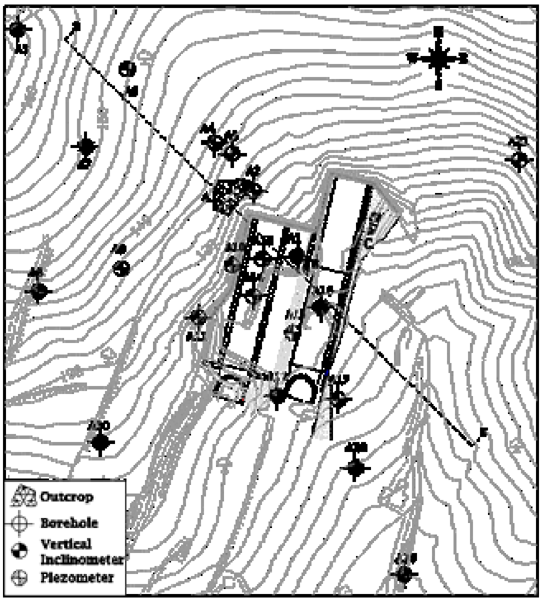


Figure 1 Investigated area and location of the boreholes and of the instruments.

The planned retaining structure consists of a multi-anchored "reverse W"-shaped wall connecting the two tunnel portals, which are longitudinally displaced about 30 m (see plan view of Figure 1). The tunnel direction is N-S so that the west wall wing is the most exposed to the effects of slope instabilities. The wall consists of 98 large diameter (D = 1200 mm) reinforced concrete piles, spaced at 1500 mm, retained with three levels of temporary anchors, 26 to 31 m long.

### 2.2 Monitoring and investigations

The landslide evolution has been followed through an extensive monitoring network (Fig. 1) which needed to be progressively updated during the construction works because of the frequent loss of instruments and the widening of the investigated area. The monitoring provided from the beginning of the excavation works (September 2007) for the retaining portal structures is a precision detection of the displacements of the top beam through in-place optical targets. When the first unexpected displacements occurred, a set of three boreholes were drilled along the slope in alignment with the dipping direction, up to a depth varying between 30.0 and 52.0 m from the ground level and instrumented with inclinometer tubes. The results of such monitoring showed the presence of a planar, block type, sliding surface at about 20 m from the surface. Since April 2010, a new site investigation was initiated to highlight the kinematics and the time evolution of the observed landslide phenomenon.

A new series of boreholes were drilled in the slope, widely distributed both inside and outside the assumed landslide area, instrumented with both electric piezometers and inclinometers. The continuous corings were examined on site in order to define the soil stratigraphy and to identify any relevant geological feature. Undisturbed samples inside the landslide area were taken. In addition to the boreholes, a series of CPTu's were carried out in the portal area and uphill.

Moreover, two mapping windows were chosen on outcrops above the wall and close to the portal, between the two pipes, in order to inspect and collect the geological essential features at a wider scale.

### 2.3 Geological setting

The lithotype found in the whole area belongs to the marine pliocenic deposits formed in a typical fan delta environment. It is constituted of the alternation of stiff overconsolidated silty clays and clayey silts with silty sandy strata, rich in microfossils, from 0.1 m to 1 m thick.

The dip direction of the strata in the landslide area is 120-140° and their inclination is about 20°. The main geological structures are associated to extensional type tectonics.

## 3 The slide at Baldaia: data interpretation

### 3.1 Monitoring data

Before the excavation of the portal was initiated, the only data available was that of topographic monitoring. Of the original 16 targets (Fig. 2), a reduced number functioned during the whole excavation period; these provided a precious tool to understand the progression of the landslide.

The observed trend from the targets indicates that the slide activated after the completion of the portal excavation, when the second level of anchors was fully installed. This is shown in Figure 2 by the rapid increase of the displacements in May 2008 when the tunnel face was still 150 m behind the portal. After a first acceleration, the displacement rate decreased during the following summer (from July to September) and then increased again at the end of November during a heavy rainfall period. In particular, the displacement patterns for targets T1, T2 and T3 show that a failure stage was reached. After these events the third level of anchors was also completed, but a significant decrease of the displacement rate for the targets could only be obtained with the earth refilling of the excavated area.

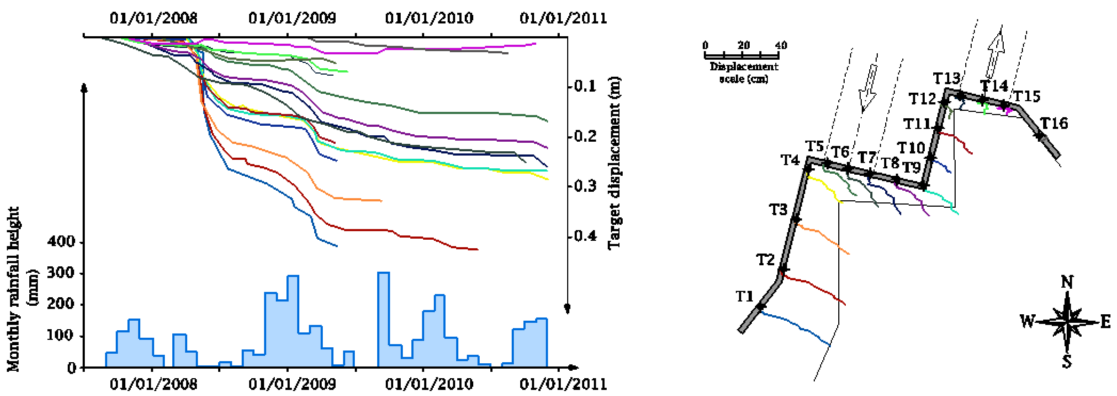


Figure 2 Top beam target displacements and monthly rainfalls during the portal construction (left); XY displacement patterns of the targets (right).

This remedial measure proved to be effective although a displacement increase is still observed especially during heavy rainfall periods. Meanwhile, the downslope Northbound carriageway was completed and the Southbound tunnel face was brought to about 30 m from the portal, close to the edges of the prospected slope instability mechanism. The XY displacement patterns of the portal top beam targets shown in Fig. 2 are characterized by a twofold trend:

- a rigid translation along the strata dip direction;
- a rigid rotation about the north carriageway portal.

In recent observations both these displacement trends are effective, although the translation component prevails.

Inclinometer profiles are shown in Fig. 3. The presence of multiple sliding mechanisms is evident, coherently with the bedding at different depths and along the slope.

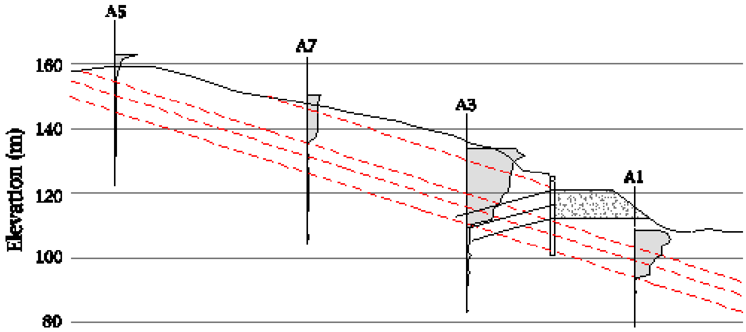


Figure 3 Inclinometer readings along the bedding planes' dip direction (S-S).

A comparison between displacement measurements from the targets and inclinometer profiles revealed how the slipping rate is governed by the deep seated surface running below the portal structures. In this sense, the Baldaia landslide may be defined as a composite landslide with the superimposition of a shallow earthflow downslope (in the first 4 m) and of three nested block-type failure mechanisms the deeper of which is located at a depth of 23 m from the surface.
The water level along the slope is fairly constant during the year and located at a depth of 20 m, rising close to the surface only at the portal yard, where the steepness of the slope progressively reduces.

### 3.2 Soil stratigraphy and soil geotechnical properties

The soil stratigraphy is well represented by a typical borehole log in Fig. 4; within the investigated depth of 45 m it appears characterized by the diffuse presence of the overconsolidated clay formation that is however interlaid by three sandy layers which were recovered at depths of 3, 10 and 32 meters from the top. CPTu profiles are also shown in Fig. 4. These profiles are very useful to detect shear planes, through a drop of both the point resistance and of the driving induced pore water pressure increment. Despite the lenticular nature of the depositional environment, the interlaid sandy layers appeared continuous at the slope scale (Fig. 5).

Through a detailed study of the recovered cores the sandy layers were identified along the entire slope, establishing their thickness and producing a picture of the structural features at the core scale. The core deformation features were observable inside the clayey layers and consisted of scaly fabric and slickenside shear planes.

Samples from the coring of a borehole inside the landslide were taken and the profile of the water content with depth was produced. Failure in overconsolidated clays is usually accompanied by the swelling and the remoulding of the soil in the shear zone, with substantial changes of the water content from the intact conditions (Henkel, 1956). This was not observed in this case, since the natural water content profile remains close to the plastic limit across the sliding surface (-22 m) without any evidence of the presence a remoulded and wet zone. The latter finding was also confirmed by pocket penetrometer tests on discontinuity surfaces which indicated undrained strength values of about 500 kPa, which is comparable with that of the intact soil.

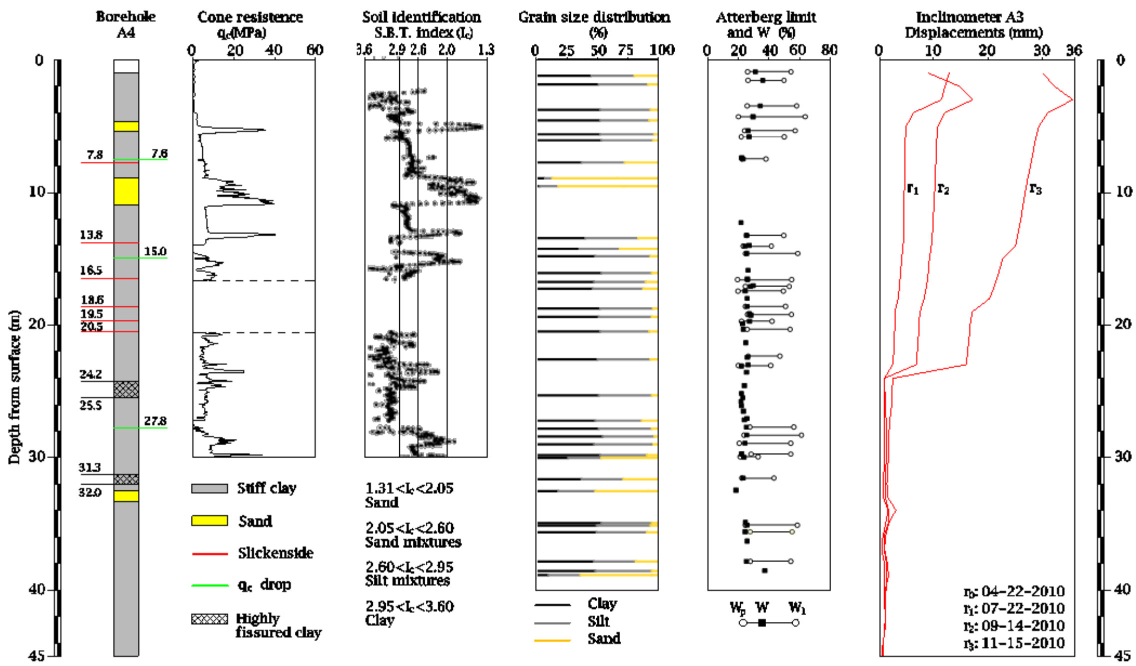


Figure 4 Overlap of data collected at the A4 borehole and the readings of the corresponding A3 inclinometer.

## 3.3 Structural characterization

The presence of macrostructures such as joints and slickensides suggests the influence of such tectonic-induced shear surfaces in the slope kinematics and indicates that a hybrid soil-rock mechanics approach should be followed for their geometrical and mechanical characterization.

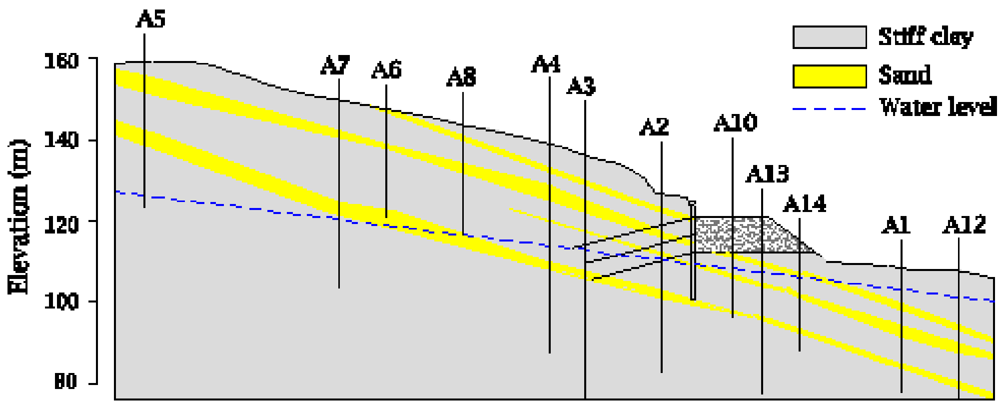


Figure 5 Location of the boreholes for slope stratigraphy.

Discontinuity characterization was carried out on different outcrops located close to the site, the main of which are above the portal and between the two carriageways. The excavated surfaces showed the frequent presence of shear bands, typical of ductile shear zones. The observed macro-structures are shown in Fig. 6 and may be interpreted as bedding planes (K1) and Riedel-type extensional shear planes (K2). Riedel shear zones typically develop as sets of conjugate second-order discontinuities in response to the stresses associated with a first-order failure in simple shear.
These structures develop at a late stage of the shearing, well after the reorientation of the minerals along the shear surface has occurred. The Riedel shear surfaces are confined between the bedding planes, exhibiting the typical S-shape within the clay layers. Only occasionally do the discontinuities cross minor sandy strata developing between the main bedding layers.
Shmidt equal area lower hemisphere stereographic projections allow to recognize the presence of five discontinuity families (Fig. 7):

- K1 bedding planes dipping 135/18° spaced from 10 to 150 cm;
- K2s “synthetic” Riedel shear planes 085/32°;
- K2a “antithetic” Riedel shear planes 090/75°;
- K3 sub vertical joints 065/85° or 248/82°;
- K4 joints dipping inside the slope 300/64°, at a right angle to the bedding planes.

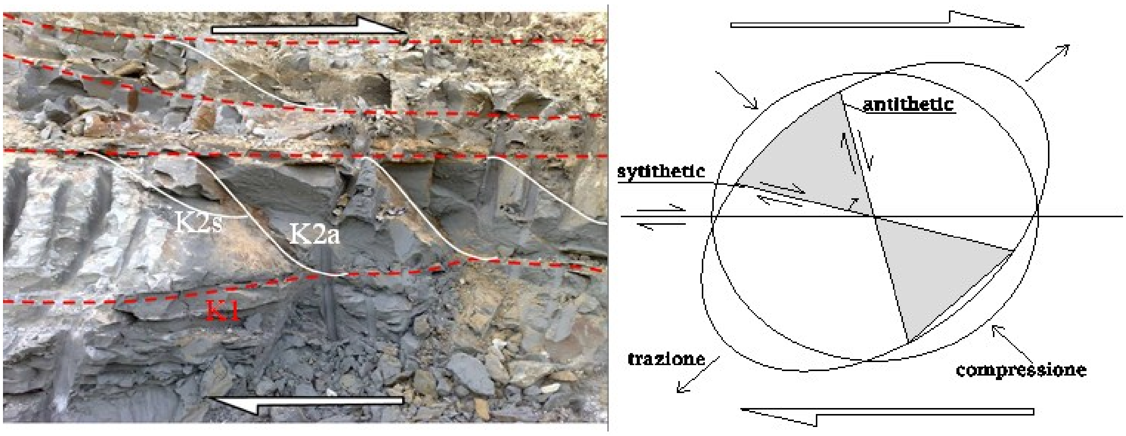


Figure 6 Riedel shear bands (white) and bedding planes (red).

The outcrop between the two carriageways exhibited a slight clockwise rotation and steepening of the K1 and K2 discontinuity sets. The former rotation may be related to the presence of a fault dislocating a 50 cm thick sand layer. The fault orientation, also observed during the excavation of the tunnel for the North carriageway, is consistent with the K4 joint family and constitutes a kinematically favourable closure plane for the main block failure. During the main outcrop cleaning operations some small blocks broke off along K3 and K4 joints, slipping in a plane-type mode along the Riedel “synthetic” shear planes K2s (Fig. 7).

At a slightly bigger scale, the whole outcrop face (10 m large and 4 m high) became later unstable, sliding along the bedding plane K1; again, K2 and K3 open tension cracks were observable 25 m uphill; the nearby inclinometer detected displacements at a depth of 5 m.


Figure 7 Different scale block detachments at the main outcrop.

Both these observed plane-type phenomena are kinematically allowable, according to the plane failure condition suggested by Hoek & Bray (1981), on the Markland test plot (Markland, 1972, Fig. 8) although their occurrence requires a friction angle along the sliding surface less than 32° for K2s plane and 18° for K1 bedding planes.

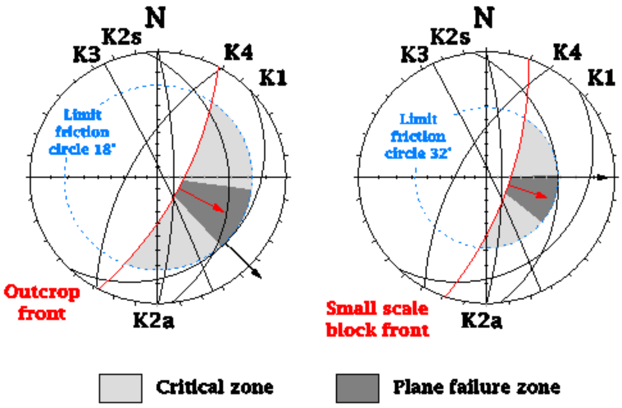


Figure 8 Stability condition on outcrop front and small scale block front.

### 3.4 Geotechnical model

The observed pattern of discontinuities, in combination with the knowledge of slope displacements from inclinometer readings, which are consistent with the aforementioned kinematic scheme, allow to define the geotechnical reference model of the entire slope (Fig. 9).

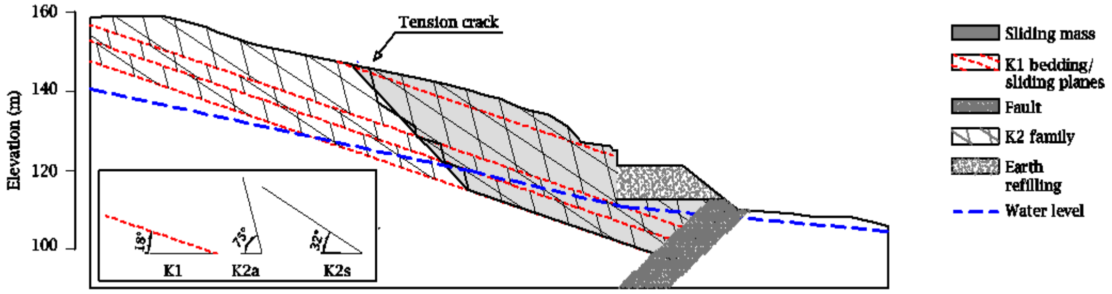


Figure 9 Proposed geotechnical model.

The unstable soil mass is thus bordered by a K1 plane, a traction K2 surface and a closing fault surface. Being the mass stability strictly related to shear strength along the discontinuities, a number of shear tests were carried out on samples containing either pre-existing discontinuities or artificially created sliding planes. Direct shear tests on 6x6 cm samples were conducted with the sliding parallel to the surfaces at a displacement rate of 1 x $10^{-3}$ mm/min. The residual strength was determined using three different procedures:

A. running 5 shearing cycles for intact samples;
B. shearing along existing surfaces;
C. shearing along artificially smoothed planes.

The tests results are summarized in Figure 10.

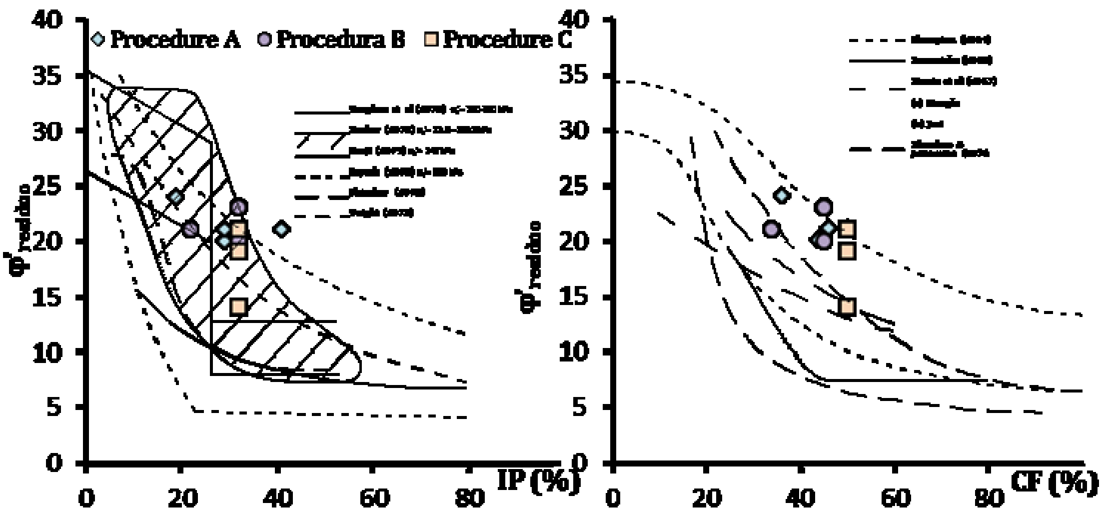


Figure 10 Summary of the residual shear tests results (after Lupini et al., 1981)

Regardless of the shearing procedure, the residual friction angle always resulted close to 20°. This value is coherent with the values of residual angle that can be inferred from classical correlations, for plasticity index (Ip) values between 20 and 30.

It is interesting to observe that with such values of residual friction, limit equilibrium analysis of the sliding block cannot by itself justify the observed instability phenomenon. Bearing in mind the results of the Markland test (Fig. 8), instability can develop only with a friction angle equal or less than 18°. Therefore an external force is needed for the instability to happen.

A closer look at the displacement vs. time graph (Fig. 2) shows the tendency of displacements to accelerate during periods of heavy rain. This fact, together with the established presence of open tension cracks, suggests the hypothesis that the cleft pressure exerted by water penetration into the open fissures may act as the triggering external force.

## 4 NUMERICAL MODEL

The stability analysis based on the limit equilibrium method show security factors slightly higher than the unity in the configuration corresponding to the end of the excavation works.

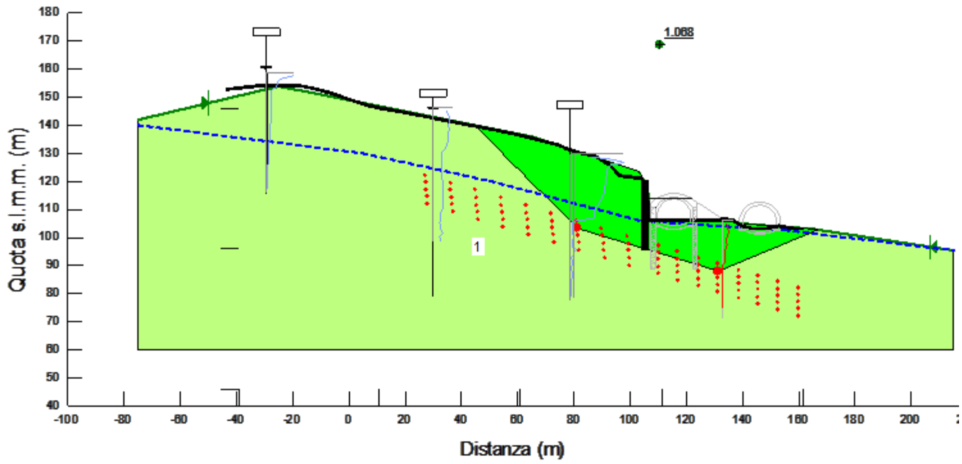


Figure 11 Sliding surface configuration at the end of the excavation

In order to interpret the monitored behaviour of the slope and to examine the role of discontinuity three numerical schemes have been implemented using FEM commercial codes: the first in plane strain conditions by means of PLAXIS V8, the second in plain strain by means of Midas 2D and the third using the three-dimensional 3D Midas code .
The real problem was characterized by a complex geometry which couldn't be handled in plane strain, thus the 3D scheme was needed to understand the influence of the topographic and geometric configuration on the creation of the sliding surface where pre-existing discontinuities are absent (toe and sides).

The initial stress of the slope, characterized by overconsolidated clays, was achieved through a preload obtained by filling the ground to the crest and then removing the exceeding soil by means of five excavation steps (Fig. 12).

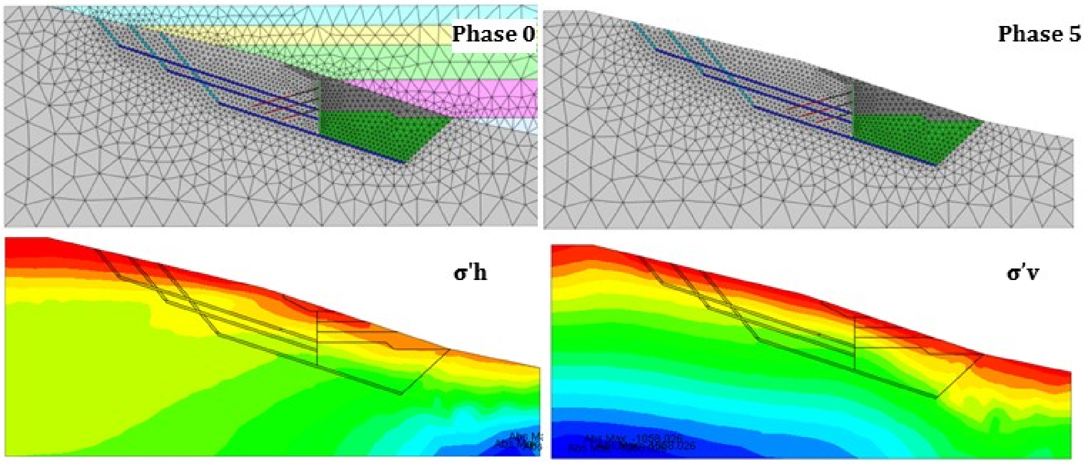


Figure 12. Simulation of the phases of erosion; horizontal and vertical in situ effective stresses

The 2D finite element analysis deformations fit the inclinometric observations, in terms of both shape and extent (block-type movement). The results of numerical analysis show also that the presence of water in the tension cracks could activate a further block located upward (secondary block) (Fig.13).

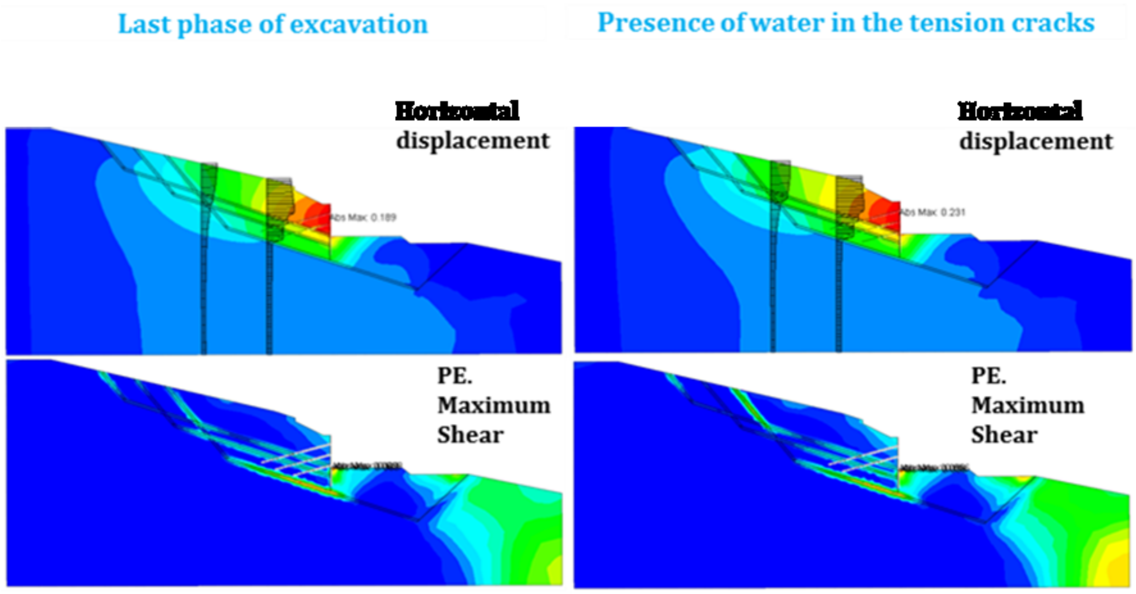


Figure 13: Main phases of the 2D modeling.

The 3D modelling substantially confirms the results of the 2D modelling, as shown in fig. 14.
The tridimensional analysis make possible to read the evolution, in terms of main direction, of the displacements of the portal structure (Fig.15). Except for the last excavating phase, the displacement directions are perpendicular to the portal, while in the last phase corresponding to the maximum excavation quote, the whole portal moves along the maximum slope direction (135° to the North). A rigid translation of the principal block on a K1 joint is evident on the 3D model of figure 14.

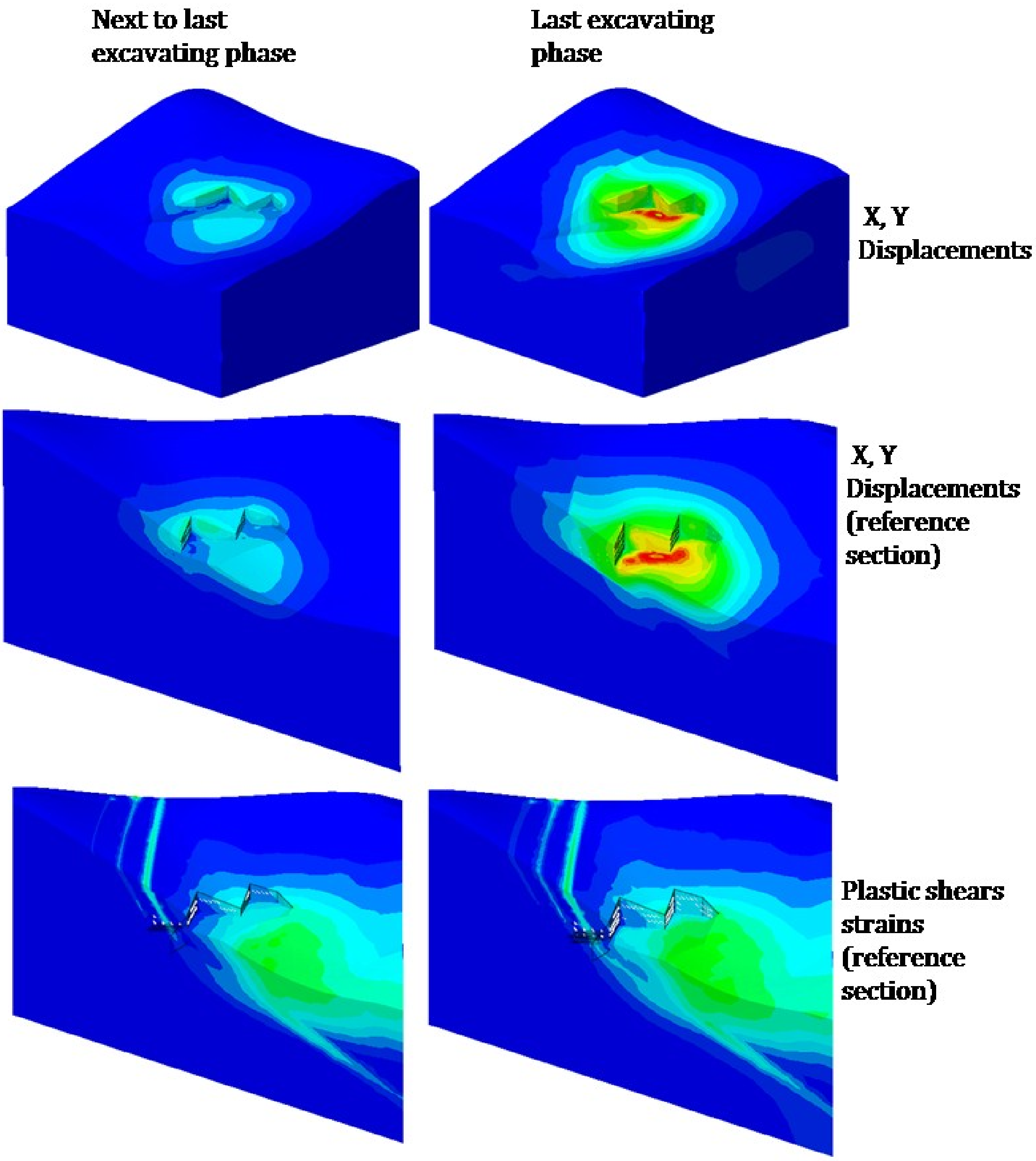


Figure 14 Main phases of the 3D modeling.

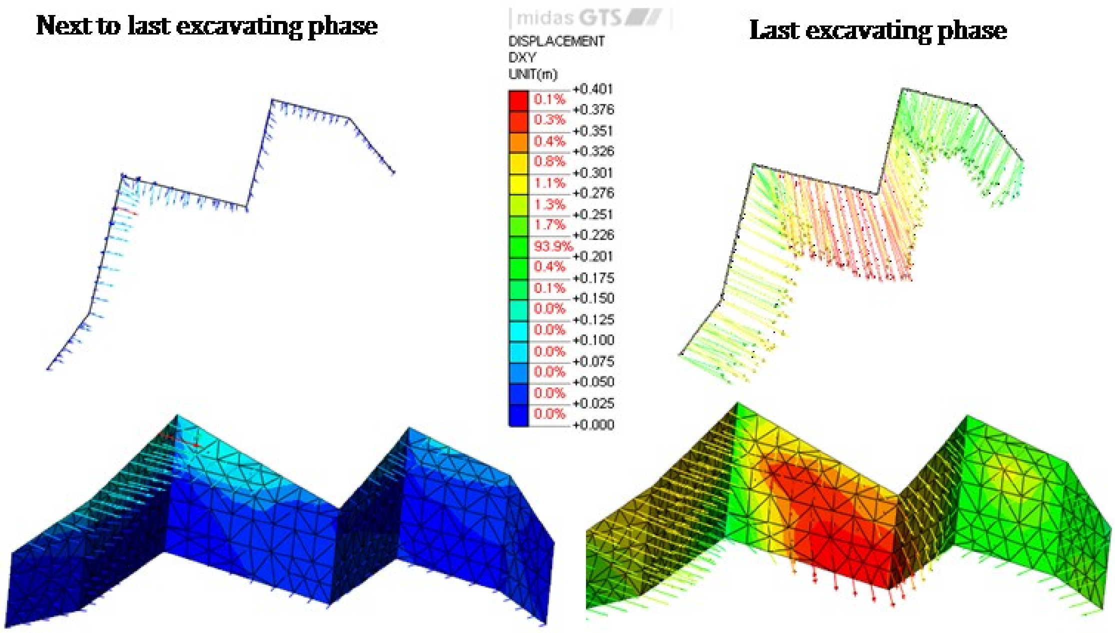


Figure 15 Displacement of the portal in the last two phases of excavation.

## 5 The tunnel completion

All the numerical analysis was run considering the block-type mass sliding along K1 bedding planes, with exit surfaces formed by K2 Riedel shear planes at the top and K4 fault joints at the toe. The block instability could be reached in the current morphologic configuration taking into account the partial tension crack filled with water. Based on this simplified model some suggestions for completion of the work were provided by running various analyses with different settings. Removal of the refilling material as well as tunnel excavation without previous loading was excluded since the resulting load reduction would lower the block safety factor.

The solution adopted was to create a retaining portal to host the future tunnel exit (Milano method), fill the whole portal area in order to gain normal stress in the passive zone and only then proceed to tunnel excavation up to the portal structure and through the filling material.

In Figure 16 a comparative view of the portal target and inclinometer displacements at the sliding depth during the completion phases is presented.

The movements of the two moving blocks, the primary and secondary, respectively, at depths of 22 m and 15 m deep, are shown in relation to different stages of progress of the tunnel face.

The block displacement speed is markedly reduced in the last tunnel excavation field due to the lower excavation induced stress relief; it gets close to zero after the completion of the artificial tunnel the occurrence of particularly intense rainfalls.

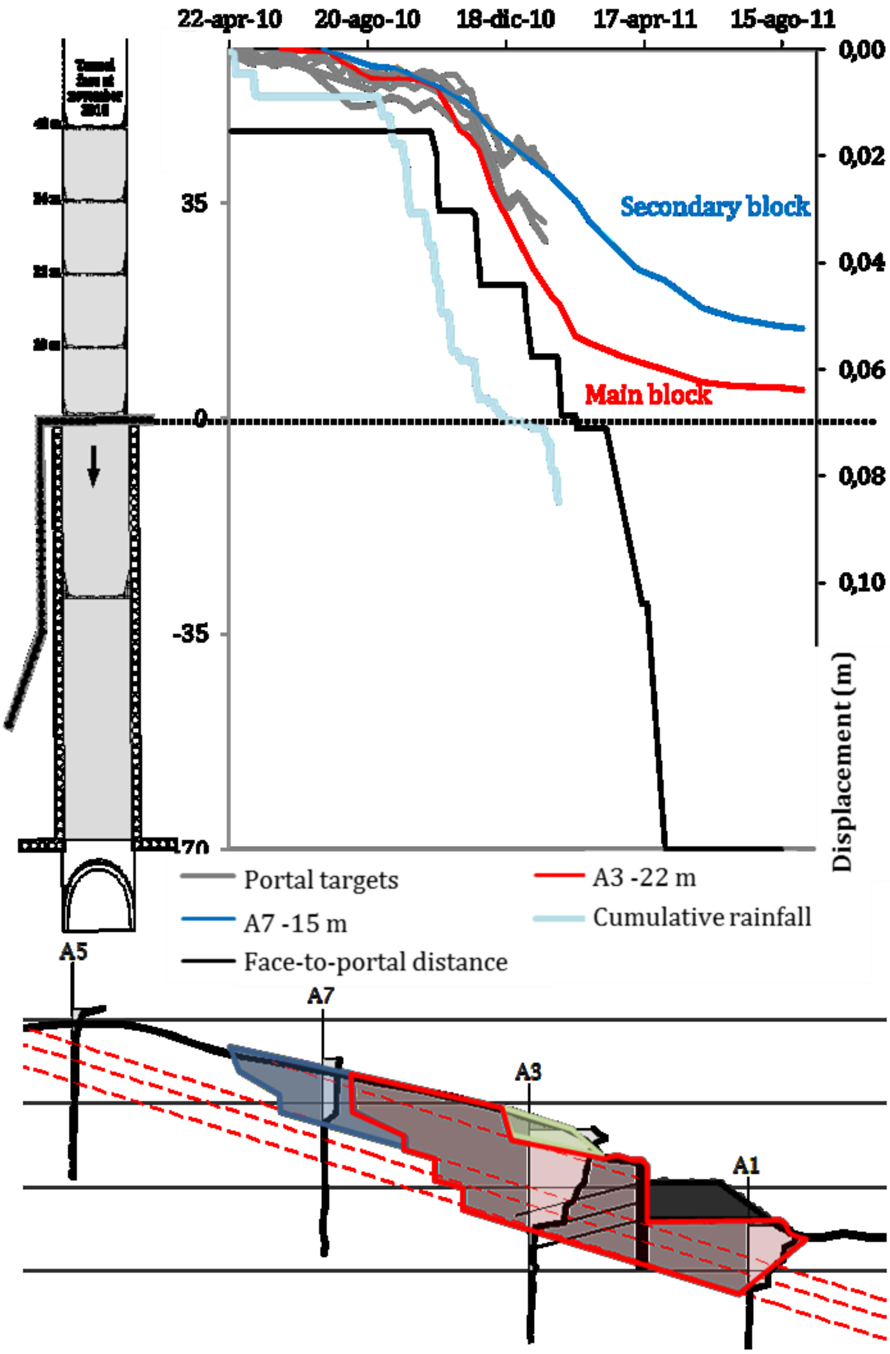


Figure 16 Comparison between portal target and deep inclinometer displacements vs southbound tunnel face-to-portal distance.

## 6 Conclusion

The reconstruction of the kinematic setup and behaviour of the soil masses within the Baldaia slope has required a comprehensive investigation and analysis of monitoring data. Tectonically induced structural features have been found to govern the movement also at large depth with shearing resistance close to the residual limit. The combination of the effects and the interaction with the construction phases and rainfall is found to be the cause of the landslide activation, along pre-existing tectonically originated discontinuities. The former results were used to build up the geotechnical reference model. Based on a block type sliding body, numerical analysis was carried out in order to guide the choices of the action to be taken to bring the tunnel to completion.

### Acknowledgments

I would like to thank Astaldi S.p.a, main contractor of the DG 21 maxi-section road construction, for making available the data used in this manuscript.

## References

[1] A.G.I. (1979) Some Italian experiences on the mechanical characterization of structurally complex formations. *Proceedings of 4th Int. Cong. on Rock Mechanics*, Montreux, vol. 2, 827-846.

[2] Calabresi G., Scarpelli G. (1985). Argille sovraconsolidate e fessurate: fenomeni franosi. *Geol. Appl. & Idrogeol.*, 20 (2): 93-126.

[3] Henkel D.J. (1956). Discussion on earth movement affecting L.T.E. *Railway in deep cutting East of Uxbridge, Proc. Institution of Civil Engineers*, Pt.II (5), 320-323.

[4] Hoek, E., Bray, J.W. (1981). Graphical presentation of geological data. Rock Slope Engineering. *Institution of Mining and Metallurgy*, Spon Press. London. (ISBN 0419160108). 368p.

[5] Lupini J.F. Skinner A. E., Vaughan P.R. (1981) The drained residual strenght of cohesive soils, *Géotechnique* 31, 181-213.

[6] Markland, J.T. (1972). A useful technique for estimating the stability of rock slopes when the rigid wedge sliding type of failure is expected. *Imp. Coll. Rock Mech. Res. Rep*. 19.

[7] Riedel W. (1929). Zur Mechanik Geologischer Brucherscheinungen. Zentral-blatt fur Mineralogie. *Geologie und Paleont.*: 354–368.